RASĀYAN *J. Chem.*
Vol. 19 | No. 4 | 1941-1947 | October-December | 2026
ISSN: 0974-1496 | e-ISSN: 0976-0083 | CODEN: RJCABP
http://www.rasayanjournal.com
http://www.rasayanjournal.co.in

GREEN SYNTHESIS OF SNO_2 NANOPARTICLES USING VARIOUS REDUCING AGENTS IN A CONTINUOUS FLOW MICROREACTOR

Sowjanya D.[1] and Sharada S.[2,✉]

[1]Department of Chemical Engineering, Jawaharlal Nehru Technological University Ananatapur College of Engineering Ananthapuramu, Research Scholar, JNTUA, Ananthapuramu.

[2]Department of Chemical Engineering, Jawaharlal Nehru Technological University Ananatapur College of Engineering Ananthapuramu-515002, Andhra Pradesh, India.

✉Corresponding author: sharadas.chemengg@jntua.ac.in

ABSTRACT

Tin oxide (SnO_2) nanoparticles were synthesised using a plant-mediated green synthesis approach. In this method, plant extracts act as effective reducing and stabilising agents, providing an environmentally friendly alternative to conventional chemical and physical synthesis routes, while minimising toxicity and biological hazards. In the present study, SnO_2 nanoparticles were prepared through a simple, low-cost, and eco-friendly process employing natural reducing agents such as ginger, *Aloe vera*, and *Acalyphaindica* leaf extracts. The entire synthesis was carried out using a continuous-flow microreactor system.

Keywords: Tin Oxide, Nanoparticles, Green Synthesis, Continuous-Flow Microreactor, Reducing and Stabilising Agent

RASĀYAN *J. Chem.*, Vol. 19, No.4, 2026

INTRODUCTION

Nanoparticles can be synthesised using eco-friendly approaches, such as green synthesis employing plant extracts.[1] Compared to conventional chemical synthesis methods, green synthesis offers significant advantages, as it avoids the use of toxic reagents and does not generate harmful by-products.[2] Enzymes, microorganisms, and plant extracts are the primary biological materials commonly employed in biosynthesis processes.[3] Among these, plant-extract-mediated synthesis is particularly attractive due to its simplicity, high efficiency, ease of operation, and low cost. In nanotechnology, nanoparticles are defined as extremely small particles that function as a single unit in terms of their transport properties and structural characteristics.[4] Tin oxide (SnO_2) exhibits excellent performance in a wide range of applications, including microelectronics, diagnostics, optoelectronic devices, biomolecular detection, and integrated electromagnetic sensors.[5] Despite the availability of various synthesis techniques, the development of SnO_2 nanoparticles through green synthesis has gained considerable attention due to its environmental compatibility and sustainability.[6] Green synthesis relies on biological precursors and is influenced by reaction parameters such as temperature, pressure, and pH.[3] Phytochemicals present in plant extracts, such as aldehydes, ketones, and phenolic compounds, play a crucial role as reducing and stabilising agents in the formation of metal oxide nanoparticles.[3] The biogenic reduction of tin ions (Sn^{4+}) into SnO_2 nanoparticles is driven by the diverse phytochemical profile of the selected extracts. In Ginger (Zingiber officinale), phenolic compounds such as gingerols and shogaols act as primary electron donors. In Aloe vera, the polysaccharide acemannan and various anthraquinones provide a high density of hydroxyl (–OH) and carbonyl (C=O) groups that facilitate both the reduction of the metal precursor and steric stabilisation of the resulting nuclei. Acalypha indica, rich in flavonoids and cyanogenic glycosides, offers a rapid reduction rate due to its high antioxidant capacity. These biomolecules form a capping layer around the SnO_2 cores, preventing excessive grain growth and agglomeration through electrostatic and steric repulsion. These metal oxide nanoparticles have found extensive applications in biomedical diagnostics, molecular sensing, humidity sensors, optical imaging, photocatalytic degradation, antimicrobial activity, and catalysis.[7]Although numerous studies have reported the green synthesis of

http://doi.org/10.31788/RJC.2026.1949767

SnO_2 nanoparticles using individual plant extracts, most investigations have been carried out using conventional batch synthesis methods. Very limited research has systematically compared the effectiveness of multiple plant-derived reducing and capping agents under identical operating conditions in a continuous-flow microreactor. Such comparative studies are essential to identify suitable plant extracts that provide enhanced nanoparticle stability, crystallinity, and morphology while benefiting from the superior heat and mass transfer characteristics of microreactor technology. Therefore, the present study addresses this research gap by comparatively investigating Aloe vera, Acalypha indica, and ginger extracts for the green synthesis of SnO_2 nanoparticles in a continuous-flow microreactor under controlled reaction conditions. Green synthesis offers a simple, economical, and environmentally friendly alternative to chemical routes for nanoparticle production.[8] Plant-mediated bottom-up approaches enable controlled nanoparticle formation using phytochemicals as reducing and stabilizing agents.[9-13] Aloe vera, rich in bioactive compounds, facilitates eco-friendly SnO_2 nanoparticle synthesis with enhanced photocatalytic and antibacterial performance.[14-23] In recent years, the development of sustainable nanomaterials has become an important research priority due to increasing environmental concerns associated with conventional chemical synthesis methods. Green synthesis using plant extracts minimises the use of hazardous chemicals, reduces waste generation, and employs renewable biological resources, making it an environmentally benign approach. Furthermore, the adoption of continuous-flow microreactor technology enhances process safety, improves heat and mass transfer, reduces reagent consumption, and provides better control over nanoparticle size and morphology compared to conventional batch synthesis.[16] Therefore, the integration of plant-mediated green synthesis with continuous-flow microreactor technology offers an efficient and sustainable strategy for nanoparticle production. This approach directly supports the United Nations Sustainable Development Goal (SDG-12): Responsible Consumption and Production by promoting eco-friendly manufacturing, efficient utilisation of natural resources, and the development of sustainable nanomaterials with minimal environmental impact.[8]

Fig.-1: *Acalyphaindica*

Fig.-2: *Acalyphaindica powder*

Fig.-3: *Aloe Vera*

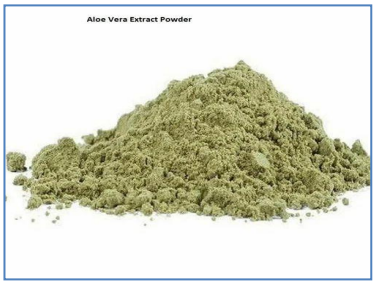

Fig.-4: *Aloe Vera powder*

Fig.-5: *Ginger*

Fig.-6: *Ginger Powder*

EXPERIMENTAL

Material and Methods

Synthesis was done in a continuous microflow reactor. Fresh leaves of *Aloe vera* and *Acalyphaindica* plucked from our institute backyard garden, and ginger was purchased from the local market of Anantapur. Tin (II) chloride dihydrate $SnCl_2 \cdot 2H_2O$ was used as the precursor material for the synthesis of tin oxide nanoparticles (SnO_2).[24] The collected leaves were initially washed thoroughly with distilled water to remove surface impurities, followed by washing with acetone. The cleaned leaves were then cut into small pieces using a sterile knife.[1] 10g of the chopped leaves/ginger was mixed with distilled water

and heated at 90 °C for 3 h to obtain the plant extract. The resulting solution was filtered using Whatman filter paper to remove solid residues, and the filtrate was stored for further use.[7] The precursor was prepared by dissolving 1.0 g of Tin (II) chloride dihydrate $SnCl_2 \cdot 2H_2O$ in 50 mL of deionized water to achieve a 0.07 M solution. This was subsequently mixed with 50 mL of the plant extract. The precursor and extract solutions were continuously fed into a microflow reactor using syringe pumps at 0.5 mL/min per syringe (Total 1.0 mL/min). The reaction was carried out at 60°C (maintained via a thermal bath) under constant temperature and flow conditions to ensure uniform mixing and controlled nucleation. The residence time within the microreactor was optimised to promote the reduction of tin ions by the phytochemicals present in the plant extracts, resulting in the formation of tin oxide nanoparticles. The residence time (τ) was calculated to be 120 seconds based on the 2.0 mL internal volume of the microchannel (ID: 0.8 mm). The initial pH of the plant extracts was measured (Ginger: 5.8, Aloe: 4.5 and Acalypha: 6.2). The reaction pH was maintained at ~8.5 using dilute NaOH to facilitate the precipitation of $Sn(OH)_4$ intermediates. The output suspension from the microflow reactor was collected and dried to obtain a thick paste. The dried product was then transferred to a porcelain crucible and calcined in a muffle furnace at 500°C for 10h to enhance crystallinity and remove organic residues.[5] After calcination, the obtained residue was finely ground using a mortar and pestle to yield SnO_2 nanoparticles.[2]

RESULTS AND DISCUSSION

XRD Analysis

XRD pattern of the SnO_2 nanoparticles synthesised using Aloe Vera extract, AcalyphaIndica and ginger extract indexed to the tetragonal rutile phase of SnO_2. The diffraction peaks correspond to the (110), (101), (200), (211), (220), (002), and (310) lattice planes, confirming the crystalline nature of the nanoparticles. The average crystallite size (D) was calculated using the Scherrer equation as 20.2 nm for ginger (Fig.-9), 32 nm for Acalypha (Fig.-8) and 32 nm for aloe vera (Fig.-7). These samples exhibited broader peaks, indicating significantly smaller crystallite sizes. The comparative XRD analysis clearly demonstrates that the plant extract significantly influences the crystallisation behaviour of SnO_2 nanoparticles. Among the three extracts, ginger-mediated synthesis produced the smallest crystallite size (20.2–25 nm)**,** whereas Aloe vera and Acalypha indica resulted in comparatively larger crystallites (32 nm). The reduced crystallite size obtained with ginger extract may be attributed to the higher concentration of phenolic compounds, flavonoids, and gingerols, which effectively regulate nucleation and inhibit excessive crystal growth. Furthermore, the controlled mixing and rapid heat transfer provided by the continuous-flow microreactor promote uniform nucleation, resulting in narrower particle size distribution and improved crystallinity. Here is an XRD graph with lattice (hkl) planes for SnO_2 (rutile structure), corresponding to your provided pattern. Assigned lattice planes (standard SnO_2-JCPDS 41-1445).

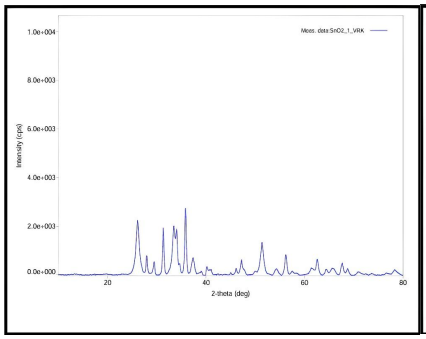

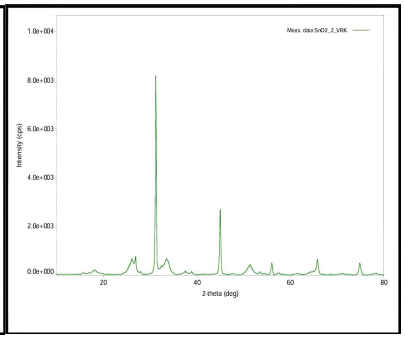

Fig.-7: - XRD of Aloe veraSnO2 NPs Fig.-8: XRD of AcalyphaIndicaSnO2 NPs

Fourier Transforms Infra-Red Spectroscopy (FTIR)

The FTIR spectra of SnO_2 nanostructures synthesised using Aloe Vera and *AcalyphaIndica* extracts were recorded over the range of 4000 cm^{-1} to 500 cm^{-1}.[3] The SnO_2 nanostructures obtained from Aloe Vera extract exhibit characteristic absorption bands at 3857, 3776, 3005, 2567, 2100, 1439, and 876 cm^{-1}, as shown in Fig.-10. In contrast, the SnO_2 nanostructures derived from *Acalypha indica* extract display bands at 3857, 2402, 1585, 1435, 875, 807, and 699 cm^{-1}, as illustrated in Fig.-11. and ginger at 3420,

1654 and 603 in Figure 12. Notably, the presence of the Sn–O functional group is confirmed by the absorption bands observed at low wave numbers, consistent with previously reported results. The FTIR spectra provide a clear comparative view of the bioactive molecules involved in the synthesis. Specifically, for the Aloe vera-derived SnO_2, the prominent peak at 1439 cm^{-1} and the series of high-wave number bands (>2100 cm^{-1}) indicate the complex interaction of acemannan and other polysaccharides with the tin surface. The clarity of the peaks and their assigned values demonstrate the purity of the sample and the effectiveness of the microreactor in maintaining consistent chemical environments during the reduction process. FTIR spectra identified the organic functional groups responsible for stabilisation. The broad band at 3400 cm^{-1} (O–H stretching) and the sharp peak at 1630 cm^{-1} (C=O stretching) confirm the involvement of polyphenols and flavonoids in the capping process. The characteristic Sn–O vibration was confirmed at lower wavenumbers (< 700 cm^{-1}), validating the formation of the SnO_2 lattice.

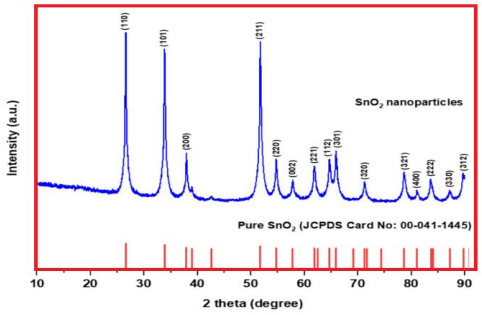

Fig.-9: XRD of Ginger SnO2 Nps

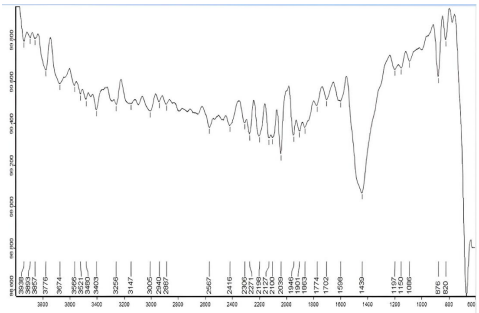

Fig.-10: FTIR of Aloe Vera SnO_2

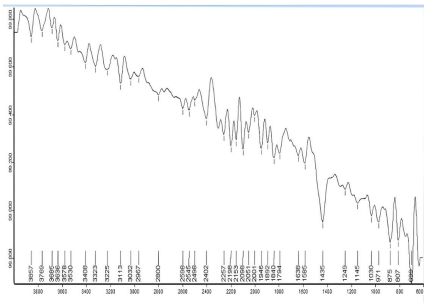

Fig.-11: FTIR of AcalyphaIndica SnO_2

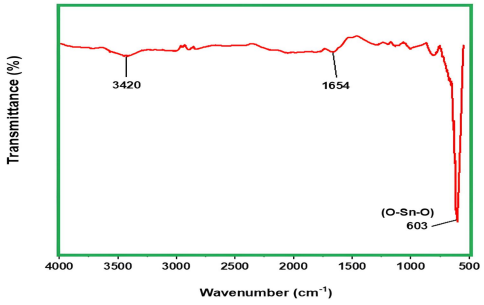

Fig.-12: FTIR of Ginger SnO_2

Comparative FTIR analysis confirms that all three plant extracts contain phytochemicals capable of acting as reducing and stabilizing agents during nanoparticle synthesis. The broad O–H stretching bands indicate the presence of hydroxyl groups originating from polyphenols and flavonoids, while carbonyl-related bands suggest the participation of biomolecules in reducing Sn^{4+} ions. The stronger and more distinct functional group interactions observed in ginger-derived nanoparticles indicate more effective surface capping, contributing to improved nanoparticle stability and reduced agglomeration.

Scanning Electron Microscopy (SEM):

The surface morphology and topological characteristics, including growth mechanism, shape, and size of SnO_2 nanoparticles, were investigated using Scanning Electron Microscopy (SEM).[4,7] SEM images of SnO_2 nanoparticles synthesised using Aloe Vera extract are presented in Fig.-13, while those synthesised with *AcalyphaIndica* extract are shown in Fig.-14.[2] The SEM micrographs reveal very fine, densely packed grains distributed uniformly across the surface. Both spherical and oval-shaped SnO_2 nanoparticles are clearly visible in the SEM images.[24] The particle size of SnO_2 nanoparticles derived from Aloe Vera extract ranges from approximately 47.06 nm to 107.6 nm; those *AcalyphaIndica* extract exhibit sizes between 53.81 nm and 112.7 nm. Whereas the ginger size 51nm shown in Fig.-15. SEM analysis revealed that nanoparticles synthesized using ginger extract exhibited a comparatively finer and more uniform morphology than those synthesized using Aloe vera and Acalypha indica. The particles

produced with ginger extract showed reduced agglomeration and a narrower size distribution, indicating efficient stabilization by the phytochemicals present in ginger. In contrast, Aloe vera and Acalypha indica extracts produced relatively larger aggregates, which may be attributed to differences in the composition and concentration of naturally occurring capping agents.

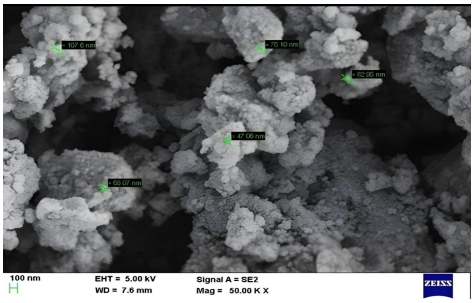

Fig.-13: SEM of Aloe Vera SnO_2

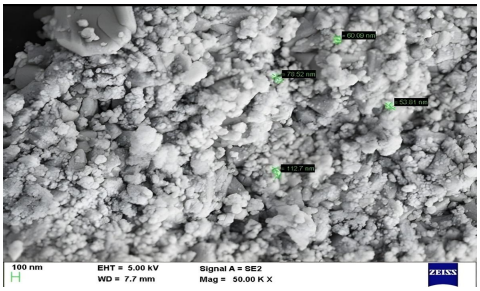

Fig.-14: SEM of AcalyphaIndicaSnO_2

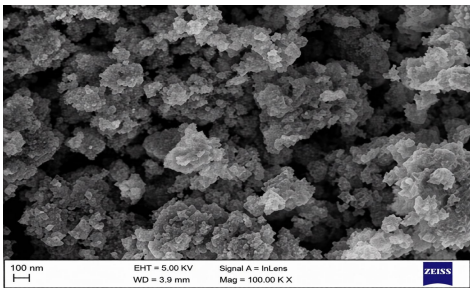

Fig.-15: SEM of GingerSnO_2

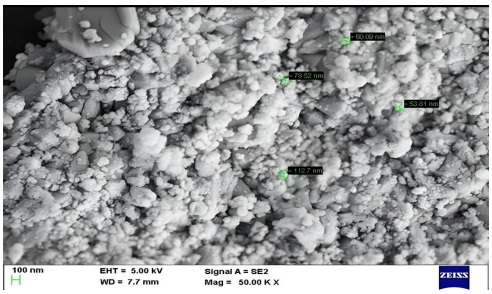

Fig.-16: TEM of Aloe Vera SnO_2

Transmission Electron Microscopy (TEM)

The HRTEM micrograph reveals distinct lattice fringes of SnO_2 nanocrystals, clearly demonstrating their crystalline structure. These spacings correspond to specific crystallographic planes of SnO_2, confirming the material's phase purity and nanoscale ordering. The sharp visibility of the fringes highlights the high degree of crystallinity present in the nanoparticles. Such direct lattice measurements provide valuable support to XRD findings, offering complementary real-space evidence of the synthesized SnO_2 nanoparticles' structural characteristics.

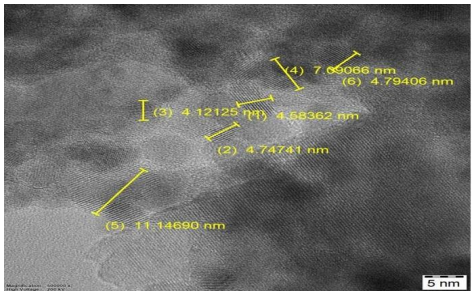

Fig.-17: TEM of AcalyphaIndica SnO_2

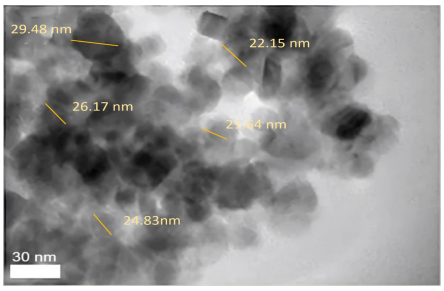

Fig.-18: TEM of Ginger SnO_2

Figure-16 represents a range from 3.48 to 4.8 nm. Figure-17 recorded spacings ranging from approximately 4.12 nm to 11.14 nm, reflecting variations across different crystallographic regions. These measurements provide direct insight into the structural ordering and nanoscale features of the material. The presence of well-defined fringes confirms the crystalline nature of the sample on the 5 nm scale bar. Figure-18 shows the average particle size 25nm, reflecting the fine distribution of crystallite dimensions within the sample. These measurements provide direct insight into the structural uniformity and nanoscale morphology of the material. TEM observations further support the XRD and SEM results. Ginger-derived SnO_2 nanoparticles exhibited smaller particle dimensions and well-defined lattice fringes, confirming

high crystallinity and uniform particle formation. The agreement between TEM and XRD analyses demonstrates that the continuous-flow microreactor provides effective control over nucleation and crystal growth. Minor differences between TEM particle size and XRD crystallite size are expected because TEM measures individual particle dimensions, whereas XRD estimates the size of coherent crystalline domains. The average particle size measured by TEM was approximately 25nm, whereas the crystallite size estimated from XRD analysis was 20.2nm. This disparity is attributed to the distinct nature of the two techniques. TEM provides direct measurement of individual nanoparticles, reflecting their actual physical dimensions, while XRD determines the size of coherently diffracting crystalline domains, which may not correspond to single particles. The larger crystallite size obtained from XRD indicates that the nanoparticles likely possess a polycrystalline structure or exist as agglomerates of smaller primary particles, causing multiple domains to diffract collectively. Furthermore, XRD represents a bulk-averaged measurement, whereas TEM analysis is based on a limited number of observed particles. Hence, the combined TEM and XRD results confirm the nanoscale nature of the synthesised material and emphasise the complementary role of both techniques in particle size and structural characterisation.

CONCLUSION

The XRD analysis indicates that the crystallite size (D) of SnO_2 nanoparticles synthesised using Aloe Vera extract is 32 nm, *AcalyphaIndica* extract is 32 nm and ginger 20.2 nm. SEM images reveal that the nanoparticles possess predominantly spherical shapes. The particle sizes observed from SEM are larger: 72.36 nm for Aloe Vera-derived SnO_2, 76.28 nm for *Acalypha indica* and ginger 51nm. FT-IR spectra of SnO_2 nanoparticles synthesised with Aloe Vera show characteristic absorption bands at 3857, 3776, 3005, 2567, 2100, 1439, and 876 cm^{-1}. In comparison, SnO_2 nanoparticles synthesised using *AcalyphaIndica* exhibit bands near 3857, 2402, 1585, 1435, 875, and 699 cm^{-1}. Ginger exhibits bands near 3368, 3305, 1647, and 1042. The crystallite sizes estimated from TEM images of Aloe Vera, *Acalypha indica* and Ginger from synthesised SnO_2, corroborate the XRD results and corresponding d-spacing values consistent with JCPDS card 41-1445. Characterisation through XRD and FTIR confirmed the successful formation of crystalline SnO_2 and the critical role of plant-derived phytochemicals in the reduction and stabilisation (capping) of the nanoparticles. Among the three investigated plant extracts, ginger exhibited superior reducing and capping capability, producing SnO_2 nanoparticles with the smallest crystallite size, enhanced crystallinity, improved morphological uniformity, and reduced agglomeration. The combination of ginger-mediated green synthesis with continuous-flow microreactor technology therefore represents a promising and sustainable approach (SDG-12: Responsible Consumption and Production) for the controlled synthesis of high-quality SnO_2 nanoparticles suitable for photocatalytic, sensing, and environmental applications.

ACKNOWLEDGMENTS

The authors are grateful to JNTUA and JNTUA CEA for allowing the facility for this work.

CONFLICT OF INTERESTS

The authors declare that there is no conflict of interest.

AUTHOR CONTRIBUTIONS

The present work is related to *SDG-12: Responsible Consumption and Production*. All the authors contributed significantly to this manuscript, participated in reviewing/editing and approved the final draft for publication. The research profile of the authors can be verified from their ORCID ids, given below:

Sowjanya D. https://orcid.org/0000-0002-4945-5538
Sharada S. https://orcid.org/0000-0002-7729-9632

Cite this article as: M. H. Wattiheluw *et al.*, *Rasayan J. Chem.*, 19(4), 1941-1947(2026), https://doi.org/10.31788/RJC.2026.1949767

REFERENCES

1. M. Nathan and P. Myvizhi, *International Journal of Pure and Applied Mathematics*, **119(12)**, 6439(2018)
2. J. Gajendiran and V. Rajendran, *International Journal of Physical Sciences and Applications*, **2**, 45(2010)
3. R. Javed, F. Nawaz, M. Sohail and I. Ahmad, *Journal of Contemporary Research in Chemistry*, **1(1)**, 42(2016).
4. D. R. Shinde, P. S. Tambade, M. G. Chaskar and K. M. Gadave, *Drinking Water Engineering and Science*, **10(2)**, 109(2017), https://doi.org/10.5194/dwes-10-109-2017
5. A. Bhattacharjee and M. Ahmaruzzaman, *Materials Letters*, **157**, 260(2015), https://doi.org/10.1016/j.matlet.2015.05.053
6. I. Hussain, N. B. Singh, A. Singh, H. Singh and S. C. Singh, *Biotechnology Letters*, **38(4)**, 545(2016), https://doi.org/10.1007/s10529-015-2026-7
7. S. Gorai, *Journal of Materials and Environmental Sciences*, **9(10)**, 2894(2018).
8. J. Singh, T. Dutta, K. H. Kim, M. Rawat, P. Samddar and P. Kumar, *Journal of Nanobiotechnology*, **16**, 84(2018), https://doi.org/10.1186/s12951-018-0408-4
9. N. Abid, A. M. Khan, S. Shujait, K. Chaudhary, M. Ikram, M. Imran, J. Haider, M. Khan, Q. Khan and M. Maqbool, *Advances in Colloid and Interface Science*, **300**, 102597(2022), https://doi.org/10.1016/j.cis.2021.102597
10. A. Hussain, N. Jabeen, I. A. Khan, M. U. Khan, M. A. Qaiser, Z. I. Zaki and M. E. Khalifa, *Crystals*, **15(1)**, 74(2025), https://doi.org/10.3390/cryst15010074
11. N. Jabeen, A. Hussain, I. Ahmad and J. Ali, ed. T. Rasheed and C. Verma, Elsevier, 2025, pp. 203–215, https://doi.org/10.1016/B978-0-443-21853-8.00012-8
12. N. Jabeen, A. Hussain, A. U. Rahman, I. Faiza, Sumbul and S. M. El-Bahy, *Solid State Ionics*, **414**, 116637(2024), https://doi.org/10.1016/j.ssi.2024.116637
13. N. Jabeen, A. Hussain, F. Shahid and M. M. Hessien, *FlatChem*, **47**, 100715(2024), https://doi.org/10.1016/j.flatc.2024.100715
14. D. Thakur, A. Sharma, D. S. Rana, N. Thakur, D. Singh, T. Tamulevicius, M. Andrulevicius, S. Tamulevicius, S. K. Shukla and S. Thakur, *Chemosensors*, **8(4)**, 108(2020), https://doi.org/10.3390/chemosensors8040108
15. D. Thakur, A. Sharma, A. Awasthi, D. S. Rana, D. Singh, S. Pandey and S. Thakur, *Chemosensors*, **8(4)**, 120(2020), https://doi.org/10.3390/chemosensors8040120
16. A. Shafey, *Green Processing and Synthesis*, **9(1)**, 304(2020), https://doi.org/10.1515/gps-2020-0031
17. Y. T. Gebreslassie and H. Gebretnsae, *Nanoscale Research Letters*, **16**, 97(2021), https://doi.org/10.1186/s11671-021-03555-6
18. S. Gowri, R. R. Gandhi and M. Sundrarajan, *Journal of Nanoelectronics and Optoelectronics*, **8(3)**, 240(2013), https://doi.org/10.1166/jno.2013.1466
19. S. Srujana, M. Anjamma, Alimuddin, B. Singh, R. C. Dhakar, S. Natarajan and R. Hechhu, *Adsorption Science & Technology*, **2022**, Article ID 7244006(2022), https://doi.org/10.1155/2022/7244006
20. S. Gautam, K. Tomar, A. S. Tomar, S. Chauhan, A. Sarkar and N. Gupta, *Inorganic Chemistry Communications*, **169**, 113126(2024), https://doi.org/10.1016/j.inoche.2024.113126
21. K. Khaldoune, N. Fdil and M. Ait Ali, *Biocatalysis and Agricultural Biotechnology*, **57**, 103052(2024), https://doi.org/10.1016/j.bcab.2024.103052
22. R. E. Abdelhameed, H. S. Hegazy and H. Abdalla, *BMC Plant Biology*, **25**, 221(2025), https://doi.org/10.1186/s12870-025-06194-6
23. R. M. S. Attar, K. M. Alkhamis, H. H. Alsharief, O. Alaysuy, K. S. Alrashdi, H. Mattar, F. Alkhatib and N. M. El-Metwaly, *Ceramics International*, **50(19, Part B)**, 36194(2024), https://doi.org/10.1016/j.ceramint.2024.07.004
24. A. Ghaderi, S. Abbasi and F. Farahbod, *Iranian Journal of Chemistry and Chemical Engineering*, **34**(4), 96(2015). [RJC-9767/2026]